

## Original Article

# siRNA targeting stathmin inhibits invasion and enhances chemotherapy sensitivity of stem cells derived from glioma cell lines

Yuwen Song<sup>1</sup>, Luyan Mu<sup>1</sup>, Xuezhe Han<sup>2</sup>, Xiaoqian Liu<sup>1\*</sup>, and Songbin Fu<sup>3</sup>

<sup>1</sup>Department of Neurosurgery, the Fourth Affiliated Hospital of Harbin Medical University, Harbin 150001, China

<sup>2</sup>Neurosurgery and Vascular Biology Program, Children's Hospital Boston/Harvard Medical School, Boston, MA 02115, USA

<sup>3</sup>Department of Genetics, Harbin Medical University, Harbin 150081, China

\*Correspondence address: Tel/Fax: +86-451-82576656; E-mail: lxq1960@hotmail.com

**Glioma is one of the most highly angiogenic tumors, and glioma stem cells (GSCs) are responsible for resistance to chemotherapy and radiotherapy, as well as recurrence after operation. Stathmin is substantial for mitosis and plays an important role in proliferation and migration of glioma-derived endothelial cells. However, the relationship between stathmin and GSCs is incompletely understood. Here we isolated GSCs from glioma cell lines U87MG and U251, and then used siRNA targeting stathmin for silencing. We showed that silencing of stathmin suppressed the proliferation, increased the apoptosis rate, and arrested the cell cycle at G2/M phase in GSCs. Silencing of stathmin in GSCs also resulted in inhibited the migration/invasion as well as the capability of vasculogenic mimicry. The susceptibility of GSCs to temozolomide was also enhanced by stathmin silencing. Our findings suggest stathmin as a potential target in GSCs for glioma treatment.**

**Keywords** stathmin; invasion; temozolomide; glioma stem cells

Received: August 5, 2014

Accepted: September 17, 2014

## Introduction

Glioma is the most common and malignant primary brain tumors in adults, which has a poor prognosis and displays unique biological features especially in the network of neoplastic blood vessels, invasion, and metastasis. The median survival time of patients with glioblastoma is still only 1 year despite positive surgery and therapy [1,2]. Tumor microvessel endothelial cells have been shown to be morphologically different from normal endothelial cells, with elevated migration and resistance to necrosis [3]. Thus, anti-angiogenesis therapy is important for glioblastoma multiforme (GBM) treatment. Previous studies have identified a small population of tumor cells called glioma stem cells

(GSCs). GSCs were first isolated in 2003 [4] and were responsible for GBM initiation, propagation, chemical therapy resistance, and glioma recurrence [5,6]. How to inhibit GSCs becomes the hot topic of glioma research.

Recently, a number of researches have demonstrated that vasculogenic mimicry (VM) plays a central role in the vascularization of GBM [7–9]. VM was an alternative vascular mechanism, which was first described and named by Maniatis *et al.* [10] in 1999. VM describes the ability of aggressive tumor cells to form vasculogenic-like networks which were associated with their high plasticity. VM is also involved in more aggressive tumor biology and can increase tumor-related mortality [11,12]. GSCs, which are the response for malignance of GBM and capable of trans-differentiation into vascular nonendothelial cells, have a strong ability of VM [13,14].

Stathmin, also known as oncoprotein 18 (OP18), is a member of the microtubule destabilizing protein family. It regulates microtubule dynamics during cell-cycle progression [15]. Most studies have demonstrated that the expression of stathmin is associated with tumor progression and unfavorable long-term prognosis. We previously reported that stathmin 1 is over-expressed in human glioma, and the inhibition of stathmin expression in high-grade glioma-derived endothelial cells significantly inhibits cell proliferation, migration, and invasion [16].

In this study, we isolated GSCs from glioma cell lines and investigated whether stathmin 1, which is extensively researched in the stathmin family, could also affect the proliferation and invasion ability of GSCs, as well as chemotherapy sensitivity to temozolomide (TMZ) to provide a potential target for anti-angiogenic treatment of glioma.

## Materials and Methods

### Cell culture and isolation of GSCs

Malignant glioma cell lines U87MG and U251 were obtained from American Type Culture Collection (Rockville, USA)

and cultured in complete Dulbecco's modified Eagle's medium (DMEM; Invitrogen Tech, Shanghai, China). Then glioma stem-like cells were successfully obtained from U87MG and U251 cell lines following the procedure described previously [4]. Identification of GSCs was carried out by western blot analysis using antibodies against stem cell markers (Oct3/4, MDR1, Sox2 and Nestin; Abcam, Cambridge, UK).

### RNA interference

The Stealth siRNA against stathmin was designed and synthesized by Invitrogen Tech. The sequences were 5'-GCUUCUUCUGAUAUCCAGGUGAAAG-3', 5'-CUUUCACCUUGGAUAUCAGAAGAAGC-3', and 5'-GAGCUGAUUCUCAGCCCUCGGUCAA-3'. GSCs grown to a density of  $1 \times 10^5$  cells/ml were transfected in duplicate with 80 nM of a siRNA pool (three siRNA duplexes) targeting stathmin. The mixture of 4  $\mu$ l siRNAs and 6  $\mu$ l lipofectamine 2000 (Invitrogen Tech) was added onto the cells after 15-min incubation at room temperature. After overnight incubation, the cells were switched to complete DMEM for 2 days. In this experiment, scramble sequence was applied as the control group.

### GSC treated with TMZ

TMZ obtained from Sigma-Aldrich Co. LLC (St Louis, USA) was dissolved in DMSO to make the stock solution at 10 mM which was then diluted into gradient concentrations. Then GSCs were cultured in 96-well plates and treated with gradient TMZ. Then LD<sub>50</sub> of TMZ on GSCs was calculated, and cell apoptosis analysis and cell cycle assay were also performed.

### Cell proliferation assay

GSCs were cultured in 96-well plates (6000 cells/well) and transfected as mentioned above. Transfected and non-transfected cells were incubated for 24, 48, and 72 h, respectively. Then cell proliferation was analyzed by MTT colorimetric assay. Experiments were performed thrice.

### Cell apoptosis assay

After treatment, cells were washed, harvested, and counted. Then  $1 \times 10^5$  cells were re-suspended in 100  $\mu$ l binding buffer and incubated in the dark for 15 min at room temperature. Finally, 10  $\mu$ l of Annexin V and 5  $\mu$ l of PI (Sigma-Aldrich Co. LLC) were added according to the manufacturer's instruction in the apoptosis kit (Biosea, Beijing, China). The apoptosis rate was determined with an Epics Altra II cytometer (Beckman Coulter, Danvers, USA). Cells were also viewed under an inverse fluorescent microscope. The experiment was repeated thrice.

### Western blot analysis

Total protein was extracted and the concentrations were measured using a spectrophotometer (Bio-Rad, Hercules, USA). Then, sodium dodecyl sulphate–polyacrylamide gel electrophoresis was performed and transferred onto PVDF membrane (Millipore, Bedford, USA), followed by blocking with skimmed milk dissolved in tris buffer saline with tween-20 (TBST) for 1 h at room temperature. The membrane was incubated with primary antibody at 4°C overnight, and incubated with HRP-conjugated secondary antibody for 1 h at room temperature after washing thrice with TBST. After washing, the bands of protein were detected with ECL substrates (ZhongShan Co. Ltd, Beijing, China).

### Cell cycle assay

After treatment, cells were harvested, washed with ice-cold PBS, and fixed with 70% ethanol at 4°C overnight. The ethanol was removed by centrifugation and  $\sim 10^6$  cells were re-suspended in PBS containing 50  $\mu$ g/ml PI and 50  $\mu$ g/ml RNase A (Sigma-Aldrich Co. LLC) for 30 min in the dark before being analyzed on a FACScalibur flow cytometer (BD Biosciences, Bedford, USA). The percentage of cells at G0/G1, S, or G2/M phase was thereby calculated. DMSO-treated cells were used as control. Experiment was repeated thrice.

### Quantitative real-time PCR

Cells were lysed with Trizol reagent (Invitrogen Tech) and total mRNA was extracted. The mRNA was reverse-transcribed into cDNA with a reverse-transcription kit (Promega Biotech). For PCR analysis, cDNA from triplicate dishes was diluted to a final concentration of 10 ng/ $\mu$ l. Quantitative real-time PCR was performed with a Universal Master Mix (Chembase, Beijing, China). cDNA (50 ng) was used to determine the relative amounts of mRNA by real-time PCR using MAX3000 Sequence-Detection System (Chambase) with specific primers and probes. The reaction was conducted for 40 cycles.  $\beta$ -actin was amplified as reference for stathmin. The primer and probe sequences are listed in Table 1.

### Transwell assay

In the invasion assay, 50  $\mu$ l Matrigel (BD Biosciences) was added to the upper chamber of the transwell apparatus with 8- $\mu$ m pore size membrane (Costar, Cambridge, USA). After the Matrigel solidified at 37°C, cells were added into the upper chamber, and the lower chamber received completed medium. Membranes coated with Matrigel were swabbed with a cotton swab and fixed with 100% methanol for 10 min after 24 h incubation. The membranes with cells were soaked with crystal violet. The number of cells attached to the lower surface of the polycarbonate filter was counted. In the migration assay, all procedures were applied without Matrigel, and

**Table 1. Primers and probes used for qRT-PCR**

Gene	Sequences
<i>Stathmin</i>	F: 5'-ACTGCCTGTCGCTTGTCT-3' R: 5'-GTCTCGTCAGCAGGGTCT-3'
<i>β-Actin</i>	P: 5'-CTTCAGTCTCGTCAGCAGG-3' F: 5'-CTCCATCCTGGCCTCGTGT-3' R: 5'-GCTGTACCTTACCCTTCC-3' P: 5'-CCAACACAGTGCTGTCTGGCGG-3'

the cell number was calculated after 12 h. Experiments were done in triplicate.

### Scratch-wound healing recovery assay

In wound healing assays, cell motility was assessed by measuring the movement of cells into a scraped area. The cells were placed in 24-well plates and scraped 2.0 mm wound with a 20  $\mu$ l pipette tip. The speed of wound closure was monitored after 12 and 24 h, and the ratio of the width of the wound versus 0 h was calculated. Each experiment was performed in triplicate.

### VM assay

Immediately before use, 24-well plates were coated with high-concentration Matrigel (200  $\mu$ l/well) and incubated at 37°C for 40 min, until the Matrigel was solid. Cells were spun down, resuspended and seeded on Matrigel-coated wells at a density of 30,000 cells per well. Human umbilical veins endothelial cells (HUVECs) were applied as reference. After incubation photomicrographs were taken for each well and the number of tubes (complete circular structures) was counted. The mean from the three readings of each well was used as the final reading.

### Statistical analysis

Statistical analyses were performed using SPSS 16.0 statistical software (SPSS, Chicago, USA), and  $P < 0.05$  was considered to show statistically significant difference.

## Results

### Stathmin silencing suppressed proliferation and induced apoptosis of GSCs

Two strains of GSCs, GSC-1 and GSC-2, were successfully obtained from U87MG and U251 cell lines, respectively (Fig. 1A). The stem cell phenotype of GSC-1 and GSC-2 was also confirmed by western blot assay, which showed that the stem cell markers Oct3/4, MDR1, Sox2, and Nestin were up-regulated in the sphere-forming GSCs compared with the adherent cells (Fig. 1B).

Application of siRNA to silence stathmin in GSCs resulted in reduced expression of stathmin at both mRNA and protein levels (Fig. 1C,  $P < 0.05$ ). Cell proliferation was significantly suppressed 24 h after siRNA transfection (Fig. 1D,  $P < 0.05$ ), whereas the rate of apoptosis was significantly increased (Fig. 1E,  $P < 0.05$ ). Consistently, pro-apoptotic proteins (Bax and cleaved caspase-3) were up-regulated, while anti-apoptotic proteins (Bcl-xl and Bcl-2) were down-regulated in stathmin-siRNA transfected GSCs (Fig. 1F).

In the group of GSCs transfected with stathmin siRNA, the percentage of cells at G2/M phase was 36.4%, compared with 13.1% in the control group (Fig. 1G), indicating that the cell cycle was arrested at the G2/M phase with stathmin silencing.

Taken together, these results demonstrated that siRNA-mediated silencing of stathmin suppresses proliferation, induces apoptosis and G2/M arrest in GSCs.

### Stathmin silencing suppressed the invasion and migratory abilities of GSCs

We performed transwell analysis to examine whether the down-regulation of stathmin affects the invasion or migratory abilities of GSCs. The results showed that the invasive and migratory capacities of GSCs were significantly inhibited by stathmin silencing. The number of stathmin-siRNA transfected cells invading through the membrane was significantly lower than that of control-siRNA transfected cells (Fig. 2A,B,  $P < 0.05$ ). Furthermore, cell migration was evaluated with a scratch-wound healing assay and the extent of cell migration into the scratched area was measured. The wounds in the wells of control-siRNA transfected cells healed rapidly and hardly a gap was left after 24 h. However, the wells of stathmin-siRNA transfected cells showed a much lower wound-healing ability than the control wells (Fig. 2C,D,  $P < 0.05$ ). These data demonstrated that stathmin silencing suppresses both the invasion and migration capacities of GSCs.

### Stathmin silencing inhibited VM of GSCs

The results of the VM assay showed both strains of GSCs had a strong ability of VM compared with the HUVEC group (Fig. 3A,B). However, the microtube formation capacity of GSCs was inhibited after stathmin-siRNA transfection (Fig. 3A); and GSCs which were transfected with siRNA formed fewer tubes compared with the control group (Fig. 3C,  $P < 0.05$ ).

### Silencing of stathmin increased chemotherapy sensitivity of GSCs to TMZ

Transfection with stathmin siRNA significantly decreased the LD<sub>50</sub> for TMZ, an alkylating agent used for the treatment of GBM, from 1052.4  $\mu$ M in control-siRNA transfected

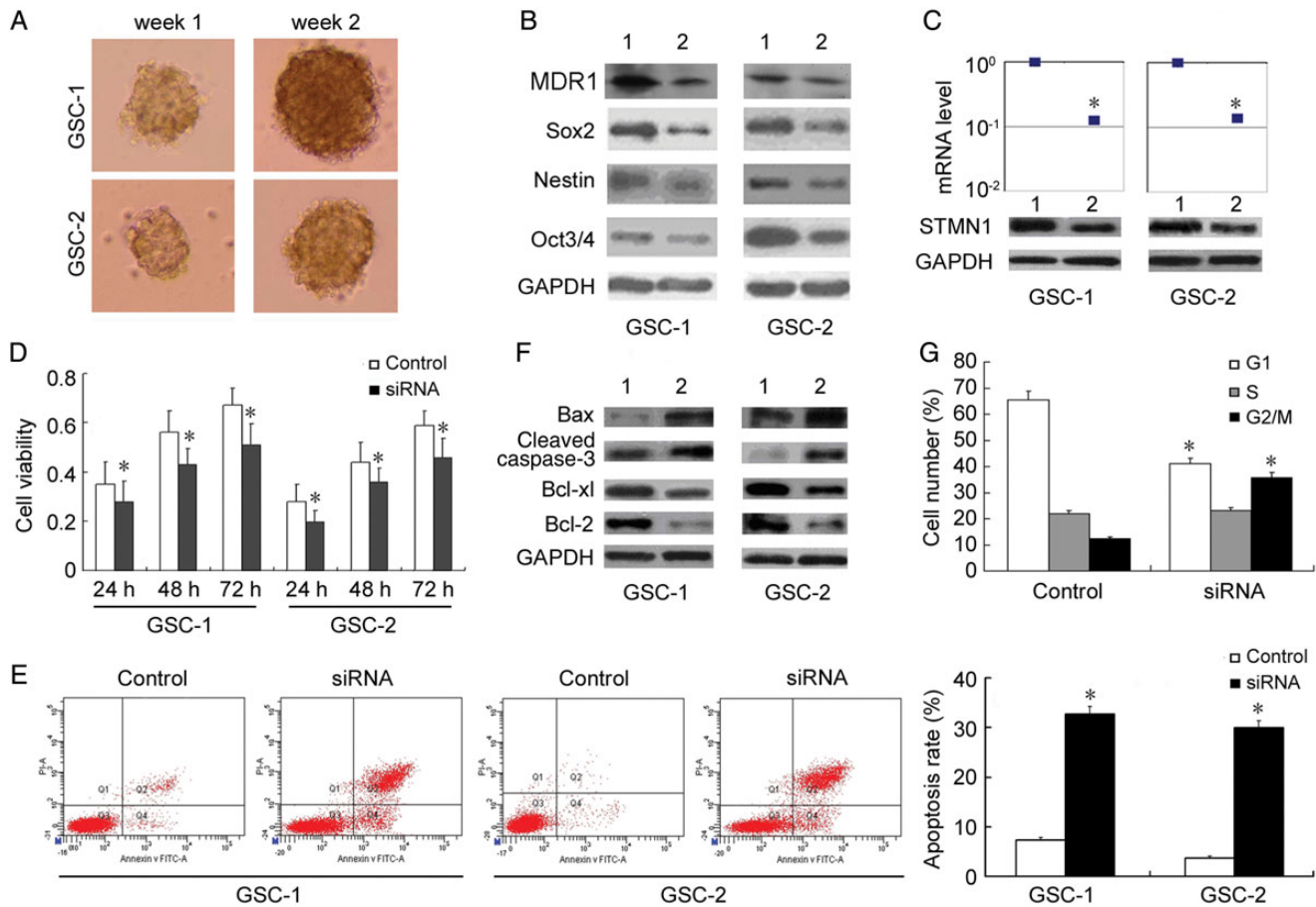


**Figure 1. siRNA target stathmin inhibited proliferation and induced apoptosis** (A) Image of GSC sphere (40×). Up panels: GSC-1 derived from U87MG cell line; lower panels: GSC-2 derived from U251 cell line. (B) Western blot analysis on stem cell markers MDR1, Sox2, Nestin, and Oct3/4. 1, sphere cells; 2, adhesion cells. (C) The stathmin mRNA and protein levels of GSCs from the two strains. mRNA level and protein level decreased after stathmin silencing. Up panel: mRNA level; lower panel: protein expression level. 1, control group; 2, siRNA group. (D) The result of MTT assay on cell viability. Cell viability of the siRNA groups was significantly lower than that of the control groups. (E) The result of cell apoptosis assay. (F) The result of western blot analysis on apoptosis proteins. Bax and cleaved caspase-3 were up-regulated while Bcl-2 and Bcl-xl were down-regulated in the siRNA group. 1, control group; 2, siRNA group. (G) The result of cell cycle assay on GSC-1. When siRNA was applied, the cell cycle was arrested at G2/M phase. Experiment was repeated thrice. \*  $P < 0.05$  vs control.

GSCs to 882.0  $\mu\text{M}$  (Fig. 4A,  $P < 0.05$ ). Stathmin silencing also significantly increased TMZ-induced apoptosis (Fig. 4B,  $P < 0.05$ ) and cell cycle arrest at G2/M phase (Fig. 4C) in GSCs. However, the apoptosis protein Bax and cleaved caspase-3 were up-regulated while anti-apoptosis protein Bcl-2 and Bcl-xl were down-regulated in the siRNA + TMZ group compared with the control group, TMZ group or siRNA group (Fig. 4D). These results demonstrated that silencing of stathmin increased chemotherapy sensitivity of GSCs to TMZ.

## Discussion

Stathmin, known as metablastin, plays an important role in malignant cancers. The activity of stathmin is regulated by phosphorylation during the cellular transition from interphase to metaphase. The non-phosphorylated stathmin

promotes the depolymerization of microtubules by sequestering tubulin [17] while the phosphorylated stathmin leads to increased microtubule stabilization and promotes the formation of mitotic spindles [18]. Stathmin is over-expressed in many malignant tumors, such as leukemia, non-small cell lung cancer, etc [19]. Stathmin over-expression can increase the invasion of prostate cancer, promote cancer progression and is associated with poor prognosis [20]. Silencing of stathmin can change the phenotype of malignant tumors, inhibit cancer cell proliferation and increase the chemotherapy sensitivity of cancer cells [21,22]. p53, which is a known tumor suppressor, can also modulate stathmin and induce cell cycle arrest at G2/M. Inhibition of stathmin in p53-mutant cell lines induces apoptosis [23]. In our previous work, we proved that stathmin expression in endothelial cells is associated with glioma WHO grade, and inhibition of stathmin suppresses proliferation,

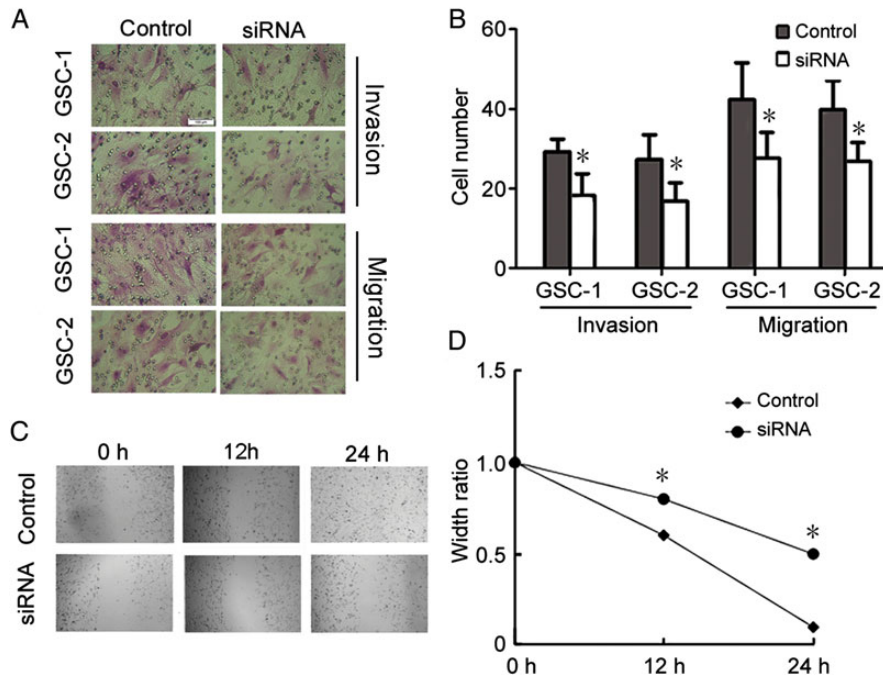


**Figure 2. siRNA target stathmin inhibited migration and invasion of GSCs** (A) The result of transwell analysis on cell invasion and migration, the cell number in the siRNA group was significantly lower than that of the control group. Upper panel: invasion assay; lower panel: migration assay. (B) The statistics of transwell assay results. Left columns: invasion assay; right columns: migration assay. (C) The result of scratch-wound healing recovery assay on GSC-2. The scratch was apparent in the siRNA group. (D) The statistics of scratch wound healing recovery assay. Experiment was repeated thrice. \*  $P < 0.05$  vs control.

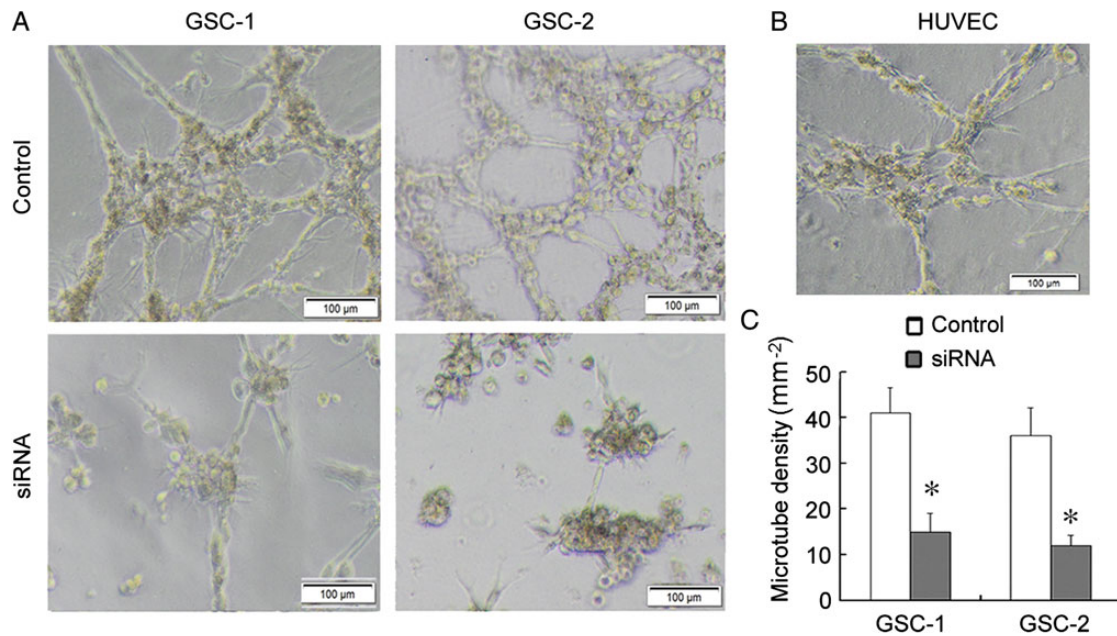


**Figure 3. siRNA targeting stathmin inhibited VM of GSCs derived from cell lines** (A) The results of vasculogenic mimicry assay, both GSCs formed abundant microtubes in control group. However, there were few microtubes in two siRNA groups. (B) HUVEC was applied as reference. (C) The statistics of vasculogenic mimicry assay. Experiment was repeated thrice. \*  $P < 0.05$  vs control.

invasion, and migration of vascular endothelial cells derived from glioma [16].

GSCs can self-renew and undergo multipotential differentiation, and are responsible for glioblastoma initiation, propagation, and recurrence [5]. In this study, we demonstrated that

silencing of stathmin could inhibit proliferation, migration, invasion, and induce apoptosis of GSCs. GSCs are also the most important reason for resistance of chemotherapy. TMZ is a kind of nitrourea that could lead to DNA mismatches which could result in cell apoptosis in GBMs [24,25]. When

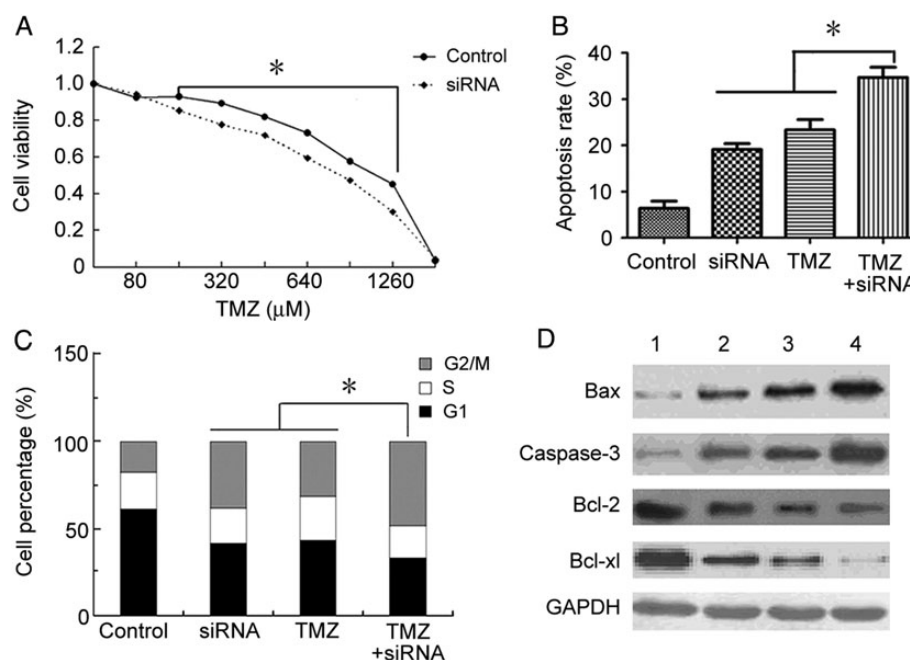


**Figure 4. siRNA targeting stathmin enhanced GSC-2 sensitivity to TMZ** (A) The result of MTT assay on cell viability of each group. (B) The result of cell apoptosis assay on each group. When siRNA and TMZ were applied together, the apoptosis rate was higher than that of the single application. (C) The result of cell cycle assay in each group. When siRNA and TMZ were applied together, the G2/M rate was higher than that of the single application. (D) The result of western blot analysis on apoptosis protein. Bax and cleaved caspase-3 were up-regulated while Bcl-2 and Bcl-xl were down-regulated in the siRNA + TMZ group compared with the control group, TMZ group, or siRNA group. 1, control group; 2, siRNA group; 3, TMZ group; 4, siRNA + TMZ group. Experiment was repeated thrice. \* $P < 0.05$  vs control.

TMZ was applied, cell cycle was arrested at G2/M phase [26]. TMZ is very effective in clinical treatment, however, TMZ application induces modest increase of life span. The existence of GSCs is responsible for TMZ resistance [27]. As our result showed that the  $LD_{50}$  of TMZ in GSCs was significantly higher than that in adhesion cells which is around  $100 \mu\text{M}$  [28]. Although application of siRNA targeting stathmin could enhance GSCs' chemical therapy sensitivity to TMZ, but the  $LD_{50}$  was still as high as  $800 \mu\text{M}$ . So how to eliminate GSCs is very important for glioma treatment.

In 1999, Maniatis *et al.* [10] were the first to report a new vascular entity named VM. The term VM has been used to describe the manner in which highly aggressive melanoma cells have the ability to form vasculogenic-like networks similar to embryonic vasculogenesis, which is independent of endothelial cells. The histological structures of VM channels are patterned networks of interconnected loops of periodic acid-Schiff (PAS)-positive extracellular matrix formed by aggressive tumor cells [29]. It is a new type vascularization of tumor that allows tumor cells to survive from hypoxia and denutrition environment. Moreover, a regular agent that targets VEGF for anti-angiogenesis therapies, such as endostar, works poorly for VM cure. In glioma, the VM-positive rate was associated with the grade of glioma, the GBM which is Grade IV has a strong ability of VM, and responsible for poor prognosis [9]. Thus developing a new way to inhibit VM may provide a potential method for GBM

treatment. GSCs could also strongly induce endothelial cell migration and proliferation [30], as well as VM [14]. In this study, we demonstrated that silencing of stathmin could inhibit VM of GSCs. Taken together with our previous work [16], our data showed that inhibition of stathmin could suppress both angiogenesis dependent on endothelial cells and VM dependent on aggressive tumor cells, which suggested that stathmin is a potential target for anti-angiogenesis and anti-GSC treatment of glioma.

Further elucidation of the mechanisms of tumor angiogenesis and GSCs may provide more precise and effective anticancer therapies. Our findings suggested that stathmin plays an important role in glioma progression by supporting neo-angiogenesis. Stathmin may be used as a novel therapeutic target molecule in human glioma.

## Acknowledgements

The authors thank Ms Shaohong Fang and Mr Jiangtian Tian from Key Laboratory of Myocardial Ischemia Mechanism and Treatment Ministry (Harbin, China) for laboratory support.

## Funding

This work was supported by the grants from the Wu Jieping Clinic Research Fund (No. 320.6750.1330) and Heilongjiang Education Fund (No. 12541304).

## References

1. Shrieve DC, Alexander E, 3rd, Black PM, Wen PY, Fine HA, Kooy HM and Loeffler JS. Treatment of patients with primary glioblastoma multiforme with standard postoperative radiotherapy and radiosurgical boost: prognostic factors and long-term outcome. *J Neurosurg* 1999, 90: 72–77.
2. Louis DN, Ohgaki H, Wiestler OD, Cavenee WK, Burger PC, Jouvet A and Scheithauer BW, *et al.* The 2007 WHO classification of tumours of the central nervous system. *Acta Neuropathol* 2007, 114: 97–109.
3. Charalambous C, Chen TC and Hofman FM. Characteristics of tumor-associated endothelial cells derived from glioblastoma multiforme. *Neurosurg Focus* 2006, 20: E22.
4. Singh SK, Clarke ID, Terasaki M, Bonn VE, Hawkins C, Squire J and Dirks PB. Identification of a cancer stem cell in human brain tumors. *Cancer Res* 2003, 63: 5821–5828.
5. Dietrich J, Diamond EL and Kesari S. Glioma stem cell signaling: therapeutic opportunities and challenges. *Expert Rev Anticancer Ther* 2010, 10: 709–722.
6. O'Brien CA, Kreso A and Jamieson CH. Cancer stem cells and self-renewal. *Clin Cancer Res* 2010, 16: 3113–3120.
7. Yue WY and Chen ZP. Does vasculogenic mimicry exist in astrocytoma? *J Histochem Cytochem* 2005, 53: 997–1002.
8. El Hallani S, Boisselier B, Peglion F, Rousseau A, Colin C, Idhah A and Marie Y, *et al.* A new alternative mechanism in glioblastoma vascularization: tubular vasculogenic mimicry. *Brain* 2010, 133: 973–982.
9. Liu XM, Zhang QP, Mu YG, Zhang XH, Sai K, Pang JC and Nq HK, *et al.* Clinical significance of vasculogenic mimicry in human gliomas. *J Neurooncol* 2011, 105: 173–179.
10. Maniotis AJ, Folberg R, Hess A, Seftor EA, Gardner LM, Pe'er J and Trent JM, *et al.* Vascular channel formation by human melanoma cells *in vivo* and *in vitro*: vasculogenic mimicry. *Am J Pathol* 1999, 155: 739–752.
11. Sun B, Qie S, Zhang S, Sun T, Zhao X, Gao S and Ni C, *et al.* Role and mechanism of vasculogenic mimicry in gastrointestinal stromal tumors. *Hum Pathol* 2008, 39: 444–451.
12. Liu Z, Li Y, Zhao W, Ma Y and Yang X. Demonstration of vasculogenic mimicry in astrocytomas and effects of endostar on U251 cells. *Pathol Res Pract* 2011, 207: 645–651.
13. Chen Y, Jing Z, Luo C, Zhuang M, Xia J, Chen Z and Wang Y. Vasculogenic mimicry-potential target for glioma therapy: an *in vitro* and *in vivo* study. *Med Oncol* 2012, 29: 324–331.
14. Ping YF and Bian XW. Concise review: contribution of cancer stem cells to neovascularization. *Stem cells* 2011, 29: 888–894.
15. Bhat KM and Setaluri V. Microtubule-associated proteins as targets in cancer chemotherapy. *Clin Cancer Res* 2007, 13: 2849–2854.
16. Dong B, Mu L, Qin X, Qiao W, Liu X, Yang L and Xue L, *et al.* Stathmin expression in glioma-derived microvascular endothelial cells: a novel therapeutic target. *Oncol Rep* 2012, 3: 714–718.
17. Leibl S, Zigeuner R, Hutterer G, Chromecki T, Rehak P and Langner C. EGFR expression in urothelial carcinoma of the upper urinary tract is associated with disease progression and metaplastic morphology. *APMIS* 2008, 116: 27–32.
18. Cassimeris L. The oncoprotein 18/Stathmin family of microtubule destabilizers. *Curr Opin Cell Biol* 2002, 14: 18–24.
19. Rana S, Maples PB, Senzer N and Nemunaitis J. Stathmin 1: a novel therapeutic target for anticancer activity. *Expert Rev Anticancer Ther* 2008, 8: 1461–1470.
20. Yuan RH, Jeng YM, Chen HL, Lai PL, Pan HW, Hsieh FJ and Lin CY, *et al.* Stathmin overexpression cooperates with p53 mutation and osteopontin overexpression, and is associated with tumour progression, early recurrence, and poor prognosis in hepatocellular carcinoma. *J Pathol* 2006, 209: 549–558.
21. Ghosh R, Gu G, Tillman E, Yuan J, Wang Y, Fazli L and Rennie PS, *et al.* Increased expression and differential phosphorylation of stathmin may promote prostate cancer progression. *Prostate* 2007, 67: 1038–1052.
22. Wang R, Dong K, Lin F, Wang X, Gao P, Wei SH and Cheng SY, *et al.* Inhibiting proliferation and enhancing chemosensitivity to taxanes in osteosarcoma cells by RNA interference-mediated down regulation of stathmin expression. *Mol Med* 2007, 13: 567–575.
23. Alli E, Yang JM and Hait WN. Silencing of stathmin induces tumor-suppressor function in breast cancer cell lines harboring mutant p53. *Oncogene* 2007, 26: 1003–1012.
24. Hermisson M, Klumpp A, Wick W, Wischhusen J, Nagel G, Roos W and Kaina B, *et al.* O<sup>6</sup>-methylguanine DNA methyltransferase and p53 status predict temozolomide sensitivity in human malignant glioma cells. *J Neurochem* 2006, 96: 766–776.
25. Kanzawa T, Germano IM, Komata T, Ito H, Kondo Y and Konodo S. Role of autophagy in temozolomide-induced cytotoxicity for malignant glioma cells. *Cell Death Differ* 2004, 11: 448–457.
26. Newlands ES, Stevens MF, Wedge SR, Wheelhouse RT and Brock C. Temozolomide: a review of its discovery, chemical properties, pre-clinical development and clinical trials. *Cancer Treat Rev* 1997, 23: 35–61.
27. Tran B and Rosenthal MA. Survival comparison between glioblastoma multiforme and other incurable cancers. *J Clin Neurosci* 2010, 17: 417–421.
28. Castedo M, Perfettini JL, Roumier T, Yskushijin K, Horne D, Medema R and Kroemer G. The cell cycle checkpoint kinase Chk2 is a negative regulator of mitotic catastrophe. *Oncogene* 2004, 23: 4353–4361.
29. Folberg R and Maniotis AJ. Vasculogenic mimicry. *APMIS* 2004, 112: 508–525.
30. Yan GN, Lv YF, Yang L, Yao XH, Cui YH and Guo DY. Glioma stem cells enhance endothelial cell migration and proliferation via the Hedgehog pathway. *Oncol Lett* 2013, 6: 1524–1530.